Journal of the Korean Physical Society, Vol. 63, No. 10, November 2013, pp. L1851∼L1854 Letters

Investigation of Light Coupling between a Semiconductor Nanowire and a Plasmonic Waveguide

You-Shin No, Jae-Hyuck Choi, Min-Soo Hwang and Hong-Gyu Park*
Department of Physics, Korea University, Seoul 136-701, Korea

(Received 10 June 2013, in final form 7 August 2013)

We report a theoretical investigation of light coupling between a semiconductor nanowire (NW) and a plasmonic waveguide. The light emitted from the NW is coupled to the waveguide and excites a symmetric plasmonic waveguide mode propagating along the top surface of the waveguide. Using numerical simulations, coupling efficiencies were calculated for various coupling structures consisting of tapered/non-tapered NWs and single-strip/double-strip gold waveguides. The highest coupling efficiency of >2.8% was obtained between a tapered NW and a double-strip plasmonic waveguide with a height of 200 nm. This study offers a new opportunity for the efficient integration of nanoscale light sources with plasmonic waveguides and enables further miniaturization of ultracompact photonic integrated circuits.

PACS numbers: 42.72.-g, 42.79.Gn, 42.82.Et
Keywords: Surface plasmon polaritons, Nanowires, Plasmonic waveguides, Coupling efficiency
DOI: 10.3938/jkps.63.1851

I. INTRODUCTION

Plasmonic devices such as lasers, waveguides, and nanoantennas are extremely attractive because the size of the devices can be reduced significantly to subwavelength scale and because multifunctional and ultracompact photonic integrated circuits can be developed using them [1–5]. In particular, various shaped plasmonic waveguides showing strong confinement of surface plasmon polaritons (SPPs) in the subwavelength-scale cross-section of the waveguides and relatively long propagation lengths of SPPs have been successfully demonstrated [6–9]. More recently, a practical plasmonic waveguide structure that enables both the generation and the propagation of SPPs has been demonstrated by combining an electrically-driven semiconductor nanowire (NW) with a double-strip plasmonic waveguide [10]. The NW has been used as an internal light source for the plasmonic waveguide. For this waveguide structure, however, further analysis is still needed to optimize the structural parameters and improve the light coupling between the NW and the waveguide.

In this work, we calculate coupling efficiencies for several plasmonic structures, which consist of a semiconductor NW and a metallic waveguide, by using the three-dimensional finite-difference time-domain (3-D FDTD) simulation method. Our systematic study provides both an understanding of light coupling between subwavelength-scale optical structures and appropriate design rules for plasmonic waveguides.

*E-mail: hgpark@korea.ac.kr; Fax: +82-2-3290-3589

II. SIMULATION METHOD

Figure 1 shows a schematic diagram of the plasmonic structure used for our calculation. One or two straight-strip gold waveguides are placed on a SiO_2 substrate, and at one end of the waveguide, a tapered or straight NW with a triangular cross section is aligned along the central axis of the waveguide. The light emitted from the NW is coupled to the waveguide and generates the SPP waveguide mode. Because the NW geometry is similar to that of the waveguide, the NW can function as an efficient internal light source for the waveguide to generate SPPs.

In our 3-D FDTD simulation, metals are modeled using the Drude-Lorentz modeling method, in which the dispersive materials over a wide range of the near-infrared spectral region are represented by the following equation [11]:

$$\varepsilon(\omega) = \varepsilon_\infty - \frac{\omega_D^2}{\omega^2 + i\gamma_D\omega} + \frac{\Delta\varepsilon_L\omega_L^2}{\omega_L^2 - \omega^2 - i\gamma_L\omega}, \quad (1)$$

where ε_∞ is the background dielectric constant at infinite frequency, ω_D and γ_D are the electron plasma frequency and the damping constant of the Drude term, respectively, and $\Delta\varepsilon_L$, ω_L and γ_L are the change in the relative

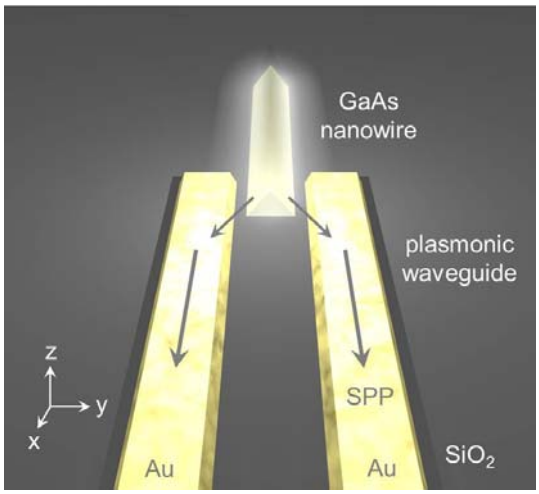

Fig. 1. (Color online) Schematic diagram of a plasmonic structure that consists of a semiconductor NW and a double-strip metallic waveguide. Light emission from the NW is coupled to the waveguide and excites an SPP waveguide mode, which propagates along the top surface of the waveguide.

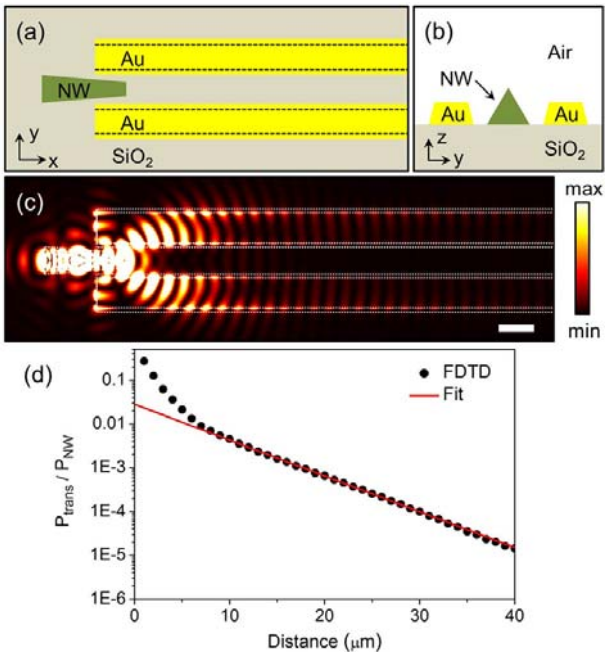

Fig. 2. (Color online) (a) Top and (b) side views of the plasmonic structure for the 3-D FDTD simulations. The NW, with a length of 2.3 μm and a triangular cross-section, is introduced as an internal light source of the double-strip gold waveguide. The length of one side of the NW gradually decreases from 700 to 400 nm. The waveguide has a trapezoidal cross-section with a height of 200 nm. A 10-nm-thick chromium layer as an adhesion layer is present underneath the gold layer of the waveguide. (c) Calculated electric field intensity distribution on the top surface of the waveguide. The scale bar is 1 μm. (d) Calculated P_{trans}/P_{NW} as a function of the distance from one end of the waveguide (black dots). A fitted curve in the range from 20 to 40 μm is also plotted (red line).

permittivity, the undamped frequency, and the damping constant of the Lorentz term, respectively. The plasma and the collision frequencies were obtained by fitting the measured refractive indices and extinction coefficients of gold and chromium over the wavelength range 700-1250 nm [12]. For gold, only the Drude term was used ($\Delta\varepsilon_L$ =0), and the parameters used in the simulation were ε_∞ = 7.26119, ω_D = 8.47319 $\hbar^{-1}$ eV, and γ_D = 0.0290695 $\hbar^{-1}$ eV, where $\hbar$ is the reduced Planck's constant. The parameters for chromium were ε_∞ = 1.01523, ω_D = 5.62522 $\hbar^{-1}$ eV, ω_L =1.98172 $\hbar^{-1}$ eV, γ_D =0.272264 $\hbar^{-1}$ eV, γ_L =3.20969 $\hbar^{-1}$ eV, and $\Delta\varepsilon_L$= 47.2679. The refractive indices of the NW and the SiO_2 substrate were set to 3.34 and 1.45, respectively [12]. In addition, a calculation domain size of 5.00 × 43.50 × 3.50 μm^3 with a spatial resolution of 10 nm was used.

To excite light emission from an NW, we introduce a dipole source with a single wavelength of 850 nm at the center of the NW. Then, we calculate the total power of the NW, P_{NW}, and the transmitted power of the SPP waveguide mode, P_{trans}, at different positions along the waveguide axis. The values of P_{NW} and P_{trans} can be obtained using the flux of the Poynting vectors passing through the surfaces, including the NW and the waveguide, respectively. The coupling efficiency between the NW and the waveguide is estimated by fitting the values of P_{trans}/P_{NW} in the middle of the waveguide and by removing the direct emission of light from the NW [10]. The extrapolated value from the fitted line of P_{trans}/P_{NW} to zero distance of the waveguide indicates the coupling efficiency. A quantitative analysis of light coupling was performed for various plasmonic structures by using this method.

III. SIMULATION RESULTS

First, we calculated the coupling efficiency between an NW and a double-strip gold waveguide (Fig. 2(a)). A 2.3-μm-long NW with a triangular cross-section was introduced at the center of the air gap of a double-strip waveguide having a semi-infinite length towards the right. The height of the waveguide was set to 200 nm, which included a 10-nm-thick chromium layer underneath the gold layer. The waveguide had a trapezoidal cross-section, and its top and bottom widths were set to 850 nm and 1.0 μm, respectively. The gap between the two strips was set to 800 nm (Fig. 2(b)). These structures of the NW and the waveguide are the same as the ones demonstrated in a previous experimental work [10]. The light emitted from the NW excites a symmetric SPP waveguide mode that propagates along the top surface of the waveguide. Figure 2(c) shows the calculated electric field intensity distribution of this SPP waveguide mode. The normalized transmitted power, P_{trans}/P_{NW}, is calculated and plotted as a function of the detection

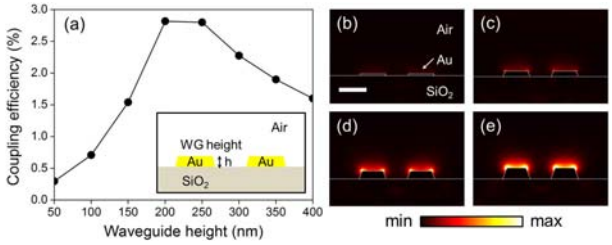

Fig. 3. (Color online) (a) Coupling efficiencies calculated as a function of the height of the double-strip plasmonic waveguide. The inset shows a side view of the NW and the waveguide. (b)-(e) Side views of the electric field intensity distributions for varying heights of the waveguide. The heights of the waveguide were (b) 100, (c) 200, (d) 300, and (e) 400 nm. These electric field intensity distributions were obtained at a 30-μm distance from the coupling region. The scale bar in (b) is 1 μm.

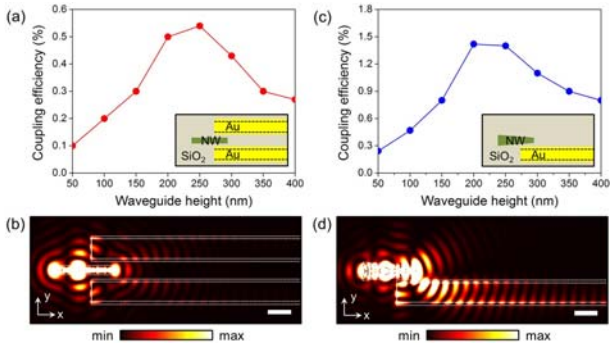

Fig. 4. (Color online) (a) Coupling efficiencies calculated as a function of the height of the waveguide and (b) electric field intensity distribution on the top surface of the waveguide with a height of 200 nm, for the structure consisting of a non-tapered NW and a double-strip plasmonic waveguide. The length of one side of the NW is 400 nm. (c) Coupling efficiencies calculated as a function of the height of the waveguide, and (d) electric field intensity distribution on the top surface of the waveguide with a height of 200 nm for the structure consisting of a tapered NW and a single-strip plasmonic waveguide. The corresponding schematic diagrams are shown in the insets of (a) and (c). The scale bars in (b) and (d) are 1 μm. The coupling efficiency in the waveguide with a height of <100 nm is slightly overestimated due to the difficulty in completely separating the direct emission of the NW from P_{trans}.

position in Fig. 2(d). The values of P_{trans}/P_{NW} decreased exponentially due to metallic absorption loss of the waveguide. The ratio P_{trans}/P_{NW} was fitted for the range from 20 to 40 μm (red line) to avoid the effect of the direct emission from the NW, which is observed at a detection position of <15 μm. Then, the coupling efficiency between the NW and the symmetric SPP waveguide mode was calculated to be ∼2.8%.

Next, to determine optimized structural parameters in the NW-coupled waveguide structure, we examined different heights of the double-strip plasmonic waveguide (Fig. 3). The coupling efficiencies shown in Fig. 3(a) were calculated using the same method as that used for the results shown in Fig. 2; they are plotted as a function of the height of the waveguide. The efficiency increases with increasing height from 50 to 200 nm whereas it decreases with increasing height from 200 to 400 nm. At a height of 200 nm, the light emitted from the NW was coupled most efficiently to the symmetric SPP waveguide mode, and its coupling efficiency was ∼2.8%, as shown in Fig. 2. Figures 3(b)-(e) represent side views of the electric field intensity distribution of each symmetric SPP waveguide mode excited in waveguides with different heights of (b) 100, (c) 200, (d) 300, and (e) 400 nm. These intensity distributions were obtained at a distance of 30 μm from the region of coupling to the NW. Even in the thick waveguides, well-guided SPP modes were observed, although their coupling efficiencies were relatively low.

The simulation result of Fig. 3(a) can be understood by considering the interaction between the NW cavity mode and the waveguide mode. Because the NW cavity mode has its maximum electric field intensity at the center of the NW cross-section and the symmetric SPP waveguide mode propagates along the top surface of the waveguide, the most efficient coupling between the NW and the waveguide is achieved when the top surface of the waveguide is at the same height as the center of the NW's cross section. As the height of the waveguide becomes larger or smaller than 200 nm, more light is coupled to the free space.

To further investigate the coupling properties, we changed the shapes of the NW and the waveguide. First, a coupling structure that included a non-tapered NW and a double-strip plasmonic waveguide was considered. In this structure, we used a 2.3-μm-long NW, which is straight along its axis and has a triangular cross-section with the length of side being 400 nm (inset, Fig. 4(a)). Other structural parameters of the waveguide remain the same as those used in Fig. 3. With these conditions, the coupling efficiency was calculated as a function of the height of waveguide (Fig. 4(a)). The entire efficiency was decreased significantly compared to that of the double-strip waveguide coupled to a tapered NW. In particular, the highest coupling efficiency of <0.6% was obtained at a height of 250 nm for the waveguide, a value that is almost one-fifth the highest efficiency value plotted in Fig. 3(a). To examine how the shape of NW influences the light coupling, we also calculated the electric field intensity distributions. Figure 4(b) shows the electric field intensity distribution obtained at the top surface of a waveguide with a height of 200 nm. We note that the emission pattern in the coupling region is considerably different from that in Fig. 2(c). The strong confinement of light in the non-tapered NW significantly reduces the coupling to the waveguide. Consequently, a relatively high optical loss in the NW can lead to a high coupling efficiency between the NW and the waveguide.

Finally, we calculated the coupling efficiency between a tapered NW and a single-strip plasmonic waveguide. This structure was constructed by simply removing one of the strips from the double-strip waveguide (inset, Fig. 4(c)). The coupling efficiencies were calculated and are plotted as a function of the height of the waveguide (Fig. 4(c)). As expected, the graph shows overall features that are similar to those for the double-strip waveguide shown in Fig. 3(a), but the coupling efficiencies are approximately decreased by a factor of two due to the removal of the single strip. This result is also supported by the calculated electric field intensity distribution, which clearly shows that only half of the light emitted from the NW couples with the waveguide (Fig. 4(d)). From these results, we can conclude that a coupled structure consisting of a tapered NW and a double-strip plasmonic waveguide with a height of 200 nm (Fig. 2) shows the best coupling efficiency.

IV. CONCLUSION

We investigated the coupling of a metal-strip straight waveguide with a semiconductor NW. The 3-D FDTD simulations showed that an NW cavity mode is coupled to a symmetric SPP waveguide mode propagating along the top surface of the waveguide. The coupling efficiencies of a double-strip gold waveguide were calculated for several heights ranging from 50 to 400 nm, and the maximum coupling efficiency was $\sim$2.8% at a height of 200 nm. In addition, a non-tapered NW and a single-strip plasmonic waveguide were examined, and their coupling efficiencies were calculated. We believe that an understanding of the light coupling that occurs between nanoscale light sources and waveguides will be useful for the practical implementation of ultracompact nanophotonic integrated circuits.

ACKNOWLEDGMENTS

This work was supported by the National Research Foundation of Korea (NRF) grant funded by the Korea government (MSIP, No. 2009-0081565). Y.-S. N. acknowledges the support of this work by the TJ Park Science Fellowship.

REFERENCES

[1] S.-H. Kwon, J.-H. Kang, C. Seassal, S.-K. Kim, P. Regreny, Y.-H. Lee, C. M. Lieber and H.-G. Park, Nano Lett. **10**, 3679 (2010).
[2] S.-H. Kwon, J.-H. Kang, S.-K. Kim and H.-G. Park, IEEE J. Quantum Electron. **47**, 1346 (2011).
[3] M.-K. Seo, S.-H. Kwon, H.-S. Ee and H.-G. Park, Nano Lett. **9**, 4078 (2009).
[4] Y. Hwang, M.-S. Hwang, W. W. Lee, W. I. Park and H.-G. Park, Appl. Phys. Express **6**, 042502 (2013).
[5] J.-H. Kang, K. Kim, H.-S. Ee, Y.-H. Lee, T.-Y. Yoon, M.-K. Seo and H.-G. Park, Nat. Commun. **2**, 582 (2011) [DOI: 10.1038/ncomms1592].
[6] S. I. Bozhevolnyi, V. S. Volkov, E. Devaux, J.-Y. Laluet and T. W. Ebbesen, Nature **440**, 508 (2006).
[7] D. K. Gramotnev, M. G. Nielsen, S. J. Tan, M. L. Kurth and S. I. Bozhevolnyi, Nano Lett. **12**, 359 (2012).
[8] R. Zia, J. A. Schuller and M. L. Brongersma, Phys. Rev. B **74**, 165415 (2006).
[9] J.-H. Kang, H.-G. Park and S.-H. Kwon, Opt. Express **19**, 13892 (2011).
[10] Y.-S. No, J.-H. Choi, H.-S. Ee, M.-S. Hwang, K.-Y. Jeong, E.-K. Lee, M.-K. Seo, S.-H. Kwon and H.-G. Park, Nano Lett. **13**, 772 (2013).
[11] A. Taflove and S. C. Hagness, Computational electrodynamics: The finite-difference time-domain method (Artech House, 2000).
[12] D. R. Lide, CRC handbook of chemistry and physics: a ready-reference book of chemical and physical data, 88th ed. (CRC Press, 2008).